POAC'23
Glasgow, United Kingdom

Proceedings of the 27th International Conference on
Port and Ocean Engineering under Arctic Conditions
12-16 June 2023, Glasgow, United Kingdom

MACKINAW (WLBB-30) ICE TRIALS 2021: ICE PROPERTIES MEASUREMENT PROGRAM

Michael Lau
National Research Council of Canada, Ocean, Coastal and River Engineering, St. John's, NL, Canada

ABSTRACT
In March 2021, the United States Coast Guard (USCG) conducted a series of ice trials with the Great Lakes Icebreaker (GLIB) Mackinaw (WLBB-30) in the Green Bay area south of Chambers Island in Lake Michigan. As part of the trials, USCG required a detailed analysis of ice strength properties in order to gain a better understanding of the impacts of ice conditions upon the cutter's equipment and performance. They approached the National Research Council of Canada (NRC) in St. John's, Canada to perform that work. This paper documents the results of this analysis. A description of the sample blocks gathered from the field, field conditions and ice specimen preparation for mechanical testing are described. The ice mechanical testing in relation with the internal structure, as observed in thin sections, is detailed with the important findings highlighted.

KEY WORDS: Ice Strength; Freshwater Ice; Great Lakes; Flexural; Compressive

INTROCTION

In March 2021, the United States Coast Guard (USCG) conducted a series of ice trials with its Great Lakes Icebreaker (GLIB) Mackinaw (WLBB-30). As part of the trials, ice sample blocks were collected. USCG required a detailed analysis of ice strength properties in order to gain a better understanding of the impacts of ice conditions upon the cutter's equipment and performance. The sample blocks were shipped to the National Research Council of Canada's (NRC) St. John's, Canada laboratory, for ice property analysis, with the ultimate objective of establishing the strength of ice encountered during the Mackinaw trials.

This paper documents the results of this analysis with a description of the sample blocks gathered from the field, field conditions, and ice specimen preparation for mechanical testing.

ICE SAMPLING AND PREPARATION

Ice Sample Harvesting Sites

The trial was conducted in the Green Bay area south of Chambers Island in Lake Michigan. Samples ice blocks were harvested from three sites and stored and organized in four insulated coolers. Sample blocks Cooler1 and Cooler3 were harvested on March 5, 2021 from two sites, respectively: Site 1, 45º 8.641’ N, 87º 23.524’ W, and Site 2, 45º 9.197’ N, 87º 23.412’ W. They had rough dimensions of 670mm x 150mm x 260mm. Cooler2 and Cooler4 were harvested on March 6, 2021 from Site 3, 45º 7.330’ N, 87º 22.289’ W, with rough dimensions of 440mm x 155mm x 225mm. Because the ice samples in Cooler2 and Cooler4 were harvested from the same site on the same day, they were expected to be very similar in structure and properties. Table 1 gives the conditions at the three harvesting sites.

Sample Preparation

The four large coolers, each containing one rough-cut ice sample block harvested from the field, were sent to NRC’s laboratory facility in St. John’s, for ice strength analysis. They were prepared shortly after reception to minimize possible crystallographic changes by storing the ice at -20ºC. The samples were also stored in plastic bags in order to minimize sublimation and they were carefully handled and shelfed to avoid crack initiation that may lead to spurious results.

Large full thickness vertical thin sections were performed on the four ice sample blocks. This operation allowed an examination of the internal structure of the samples, so as to optimize block partitioning for test specimen production. A total of 41 columns and 24 beams were prepared and tested.

Thin section observations of the sample blocks suggested the samples were harvested from the top 150mm (Site 1 and Site 2) or 100mm (Site 3) of the ice cover at the respective harvesting sites with a layer of ‘snow ice’ clearly observed, i.e. characterized by a fine-grained texture.

For all sample blocks, the top snow layer was removed prior to block partitioning. This forms a horizontal reference plane to ensure the beam and column samples produced are precisely oriented in the correct horizontal or vertical direction. For Cooler2 and Cooler4, which exhibit a T3/S1 structure (see section 4.1 for details), test specimens were produced from the ~100 mm middle layer with the horizontal reference plane located at its upper boundary. For some tests of this ice type, a limited number of bi-layer specimens were also used to examine its effect on compressive strength. These specimens were prepared by including ice material contributed from the top and center layers, and they were identified with an asterisk (see Table 3).

Table 1 Conditions at sample harvesting site 2 on March 5th

	MARCH 5TH		MARCH 6TH
	Cooler1	**Cooler3**	**Cooler2 & Cooler4**
Ice "t" [in]	19.00	21.00	20.25
Atm. Temp. [^{0}F/^{0}C]	32.00/0	36.00/2.2	35.00/1.7
Location [Lat., Long.]	45º 8.641’ N, 87º 23.524’ W	45º 9.197’ N, 87º 23.412’ W	45º 7.330’ N, 87º 22.289’ W
Temp. at 4" [^{0}F/^{0}C]	31.3/-0.4	32.5/0.3	32.2/0.1
Temp. at 8" [^{0}F/^{0}C]	31.2/-0.4	32.1/0.1	31.8/-0.1
Temp. at 12" [^{0}F/^{0}C]	31.2/-0.4	32.4/0.2	31.7/-0.2
Temp. at 16" [^{0}F/^{0}C]	31.5/-0.3	31.9/0.5	31.6/-0.2
Temp. at 19.5" [^{0}F/^{0}C]	-	32.0/0	31.7/-0.2
Ice Condition	Slight ice melt on top of sample, clear uniform ice below	Free from breaks, solid ice, no cracking, clear uniform	Clear ice, internal cracking apparent cracking apparent

Each ice specimen was machined in the cold room at a temperature of -10ºC to the required dimensions for simple beam (Figure 1) and/or unconfined uniaxial compressive testing (Figure 2). Prior to testing, the prepared ice samples from each location were allowed to stabilize for 24 hours at the "recovered test temperature" of -0.2ºC as derived from the temperatures analysis of ice cores recovered on the associated trial harvest site and day. A reference temperature of -5ºC (with a recovered test temperature of -5ºC) was also used to obtain strength data for comparison with data at the same temperature from Kirby (2007) and elsewhere.

ICE TESTING

Flexural Strength

Simple 3-point beam tests were conducted to establish the flexural strength of the ice samples at two different temperatures: one corresponded to the observed trial conditions of -0.2ºC, and the second test temperature was set to -5ºC, corresponding to the temperature selected by Kirby (2007) for ease of comparison. Several samples were created and tested at each condition. These tests were conducted on horizontal 'through thickness' samples, consistent with the 2007 test program (see Kirby, 2007). This loading direction corresponds to the loading direction of flexural loading by an icebreaking vessel. For these tests, the bottom of the ice was put in tension. The prepared ice samples were tested by loading the beam center under constant loading speed of 4 mm/s. The applied load, loading speed and beam deflection were recorded on a standard NRC data acquisition system. The reported strain rate is calculated by dividing loading speed with $S^2/(6H)$, where S is the support span and H is the sample thickness. The high strain rate ensured ductile failure of ice samples. Sixty frames per second high-definition video recordings of each test were made, which provided a means to review the failure characteristics of each test sample. See Figure 1 for the test set-up of the simple beam test.

Typical bending loads for small 'simple beam' specimens of columnar S2 freshwater ice usually range from 0.5 to 1.2 MPa (70 – 170 psi). This large range of values is normal – it is due to factors such as flaws in the ice and variations in internal structure, which is to be expected in any natural material.

Compressive Strength

Unconfined, uniaxial compressive strength tests were performed to determine the compressive strength of the ice sample (Figure 2), in both the horizontal (in-plane) and vertical (growth) axis. Ice samples for vertical tests were prepared from the sample blocks, while samples for horizontal tests were prepared from the recovered broken, but undamaged, beam specimens. Using a 20 kN (5000 lbs) Applied Test Systems Universal Testing Machine configured for cold weather deployment, with a constant loading rate of 4 mm/s, the prepared specimens were tested to failure noting applied load, loading speed, and displacement. The reported strain-rate is calculated by dividing loading speed with sample length. Again, the high strain rate ensured ductile failure of ice samples. Kirby (2007) used the same strain rate, allowing ease of comparison between these two datasets.

Figure 1 Test set-up of the simple beam test

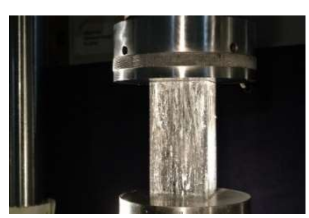

Figure 2 Prepared compressive strength test sample before testin

RESULTS AND DISCUSSIONS

Thin Sections

Through thickness vertical thin section evaluations were performed on each block using a large-scale section (LSS) technique. They show a typical S2 columnar ice structure for Cooler1 and Cooler3, and a less common T3/S1 superimposed ice with macrocrystalline structure for Cooler2 and Cooler4. Figure 3 shows the vertical thin sections for Cooler1 to Cooler4. S2 ice is the most common ice type. It is small grained columnar ice with horizontal c-axis (see Figures 3a and 3c). The primary ice (top layer) has crystals roughly 0.5 mm to 25 mm in diameter. The ice that forms underneath the primary ice layer increases in grain size with depth as crystals with a more horizontal c-axis edge out those with a more vertical one.

T3 is a layered structure of superimposed ice due to its formation process. (See Figures 3b and 3d.) It is surface ice that typically forms on puddles created by melt water, rain or moderate compression buckling of the ice sheet. T3 ice is common around pressure ridges. This type of ice is less common in the field and strength data on this type of ice are scanty. Since it has a multi-layer structure, the ~100 mm thick middle layer is used for mechanical testing.

Horizontal thin sections suggested that this layer is of the large macrocrystalline S1-type attaining cross-sectional diameters of 90 mm or more in bottom ice. Gow and Ueda (1989) reported the structure and flexural properties of this ice grown in their laboratory with comparison to the more common S2 ice.

S1 ice sheets consist of macrocrystalline ice with predominantly vertical c-axes; whereas, S2 ice is composed of vertically elongated, columnar crystals with predominantly horizontal c-axes. For detailed description of the T3/S1 and S2 ice structures and their formation processes, the readers are referred to Michel and Ramseier (1971).

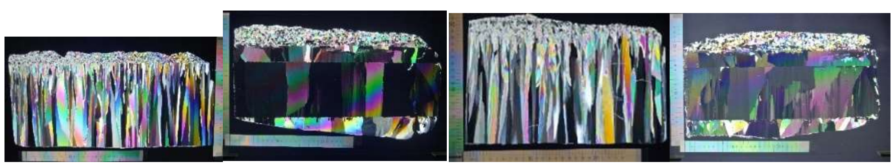

Figure 3 Through thickness vertical thin sections of ice blocks: (a) Cooler1 showing the S2 structure, (b) Cooler2 showing the T3/S1 structure, (c) Cooler3 showing the S2 structure, and (d) Cooler4 showing the T3/S1 structure. (Samples a-d are shown from left to right.

Flexural Strength

The beam tests are summarized in Table 2. Thirteen simple beams were tested at each of the targeted ice temperatures of -5 ºC and -0.2 ºC (nominal), for a total of 26 beam tests. The average span and width-to-thickness ratios were 6.1 and 1.0, respectively.

Kirby (2007) measured ice flexural strength from the Great Lakes using the same test set-up with similar sample size and ice temperature that affords direct comparison. Figure 4 shows a comparison between the present test series and Kirby (2007) flexural strength data. The data are also compared with results reported elsewhere for similar ice and test conditions as shown in Figures 5 and 6 for the S2 and S1 ice samples, respectively.

Data from S2 ice are compared with data reported by Kirby (2007), Barrette (2011), Gagnon and Gammon (1995), Gow and Ueda (1989), Murdza et al. (2020), Hitch (1959), Timco and

Frederking (1982), Lavrov (1971) and Timco and O'Brien (1994). Data from S1 ice are compared with results reported by Han et al. (2016), Gow and Ueda (1989) and Dempsey et al. (1988).

The results show a large difference in strength between the S1 and S2 ice samples. At T=-5ºC, the average flexural strength for the S1 and S2 ice samples are 4.00 ± 1.01 MPa and 1.34 ± 0.04 MPa, respectively. The S1 ice is 2.98 times stronger than the S2 ice at this temperature. At T=-0.2ºC, the average flexural strength for the S1 and S2 ice samples are 2.28 ± 0.61 MPa and 0.82 ± 0.08 MPa, respectively. The S1 ice is 2.80 times stronger than the S2 ice. Furthermore, the average ice flexural strength of 1.34 MPa obtained at -5ºC for the S2 ice specimens are comparable to Kirby's 2007 data of the same ice type, i.e., 1.21 ± 0.2 MPa, obtained at the same temperature.

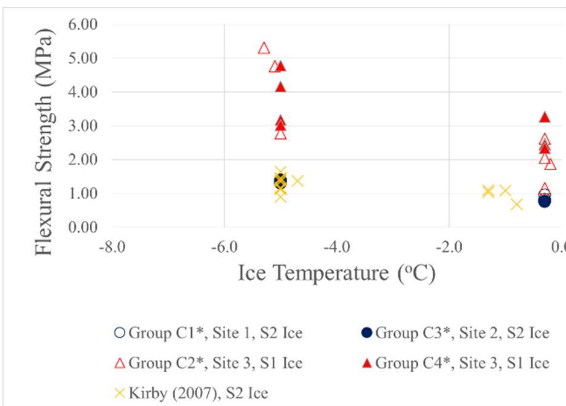

Figure 4 Flexural strength in comparison with data reported by Kirby (2007).

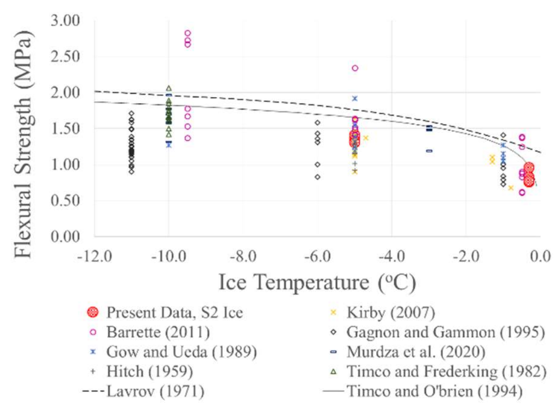

Figure 5 Flexural strength of S2 samples in comparison with data reported elsewhere on S2 freshwater ice.

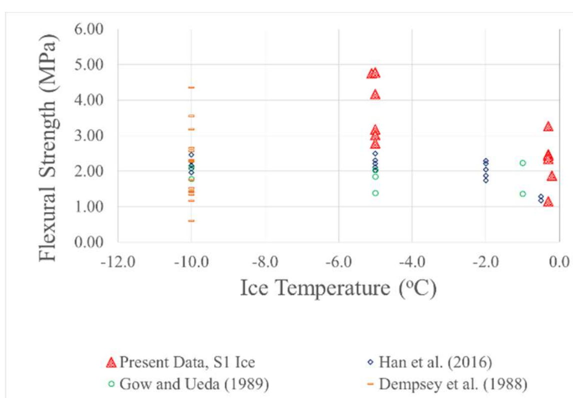

Figure 6 Flexural strength of S1 samples in comparison with data reported elsewhere on S1 freshwater ice

Table 2 Summary of flexural strength analysis on USCG Mackinaw ice samples: Loading Speed = 4 mm/s, C# – Cooler#, B# – sample beam #.

Beam Sample	Test Temp	Strain Rate	Peak Flexural Strength		Max Load	Sample Length	Support Span	Sample Thick.	Sample Width	E Modulus
I.D.	(°C)	(s^{-1})	(MPa)	(psi)	(N)	(mm)	(mm)	(mm)	(mm)	(GPa)
C1B1	-5.0	9.63E-03	1.34	195	594	443	400	64.2	64.3	3.8
C1B4	-5.0	1.17E-02	1.36	197	1061	457	400	77.8	77.5	2.3
C3B2	-5.0	1.01E-02	1.41	204	713	458	400	67.3	67.0	4.3
C3B4	-5.0	7.43E-03	1.30	189	265	459	400	49.6	49.7	6.0
C2B3	-5.3	1.44E-02	5.31	770	1212	334	275	45.4	45.7	5.3
C2B5	-5.0	1.67E-02	2.77	402	827	337	275	52.6	44.5	5.3
C2B7	-5.1	1.40E-02	4.76	690	1021	331	275	44.2	45.3	6.7
C4B1	-5.0	1.43E-02	4.78	693	1068	325	275	45.2	45.2	6.9
C4B3	-5.0	1.34E-02	3.18	461	576	332	275	42.1	42.1	6.2
C4B5	-5.0	1.46E-02	3.02	437	709	323	275	46.0	45.9	5.7
C4B7	-5.0	1.29E-02	4.17	604	673	332	275	40.6	40.4	6.1
C1B3	-0.3	9.69E-03	0.96	139	430	451	400	64.6	64.3	2.2
C1B5	-0.3	9.65E-03	0.82	119	354	449	400	64.3	62.5	3.3
C1B6	-0.3	9.83E-03	0.76	111	360	451	400	65.5	65.7	2.3
C3B1	-0.3	1.12E-02	0.76	110	525	456	400	74.8	74.4	1.4
C3B3	-0.3	9.73E-03	0.77	112	347	458	400	64.8	63.9	2.3
C2B2	-0.3	1.25E-02	2.62	380	401	335	275	39.5	40.4	4.3
C2B4	-0.3	1.55E-02	2.05	298	577	329	275	48.8	48.7	2.7
C2B6	-0.3	1.31E-02	1.16	168	199	335	275	41.2	41.8	2.5
C2B8	-0.2	1.29E-02	1.87	272	329	325	275	40.5	44.2	3.8
C4B2	-0.3	1.56E-02	2.48	359	706	328	275	49.0	48.9	4.5
C4B4	-0.3	1.51E-02	2.44	354	627	344	275	47.5	47.0	4.8
C4B6	-0.3	1.45E-02	3.27	474	755	336	275	45.6	45.8	6.5
C4B8	-0.3	1.49E-02	2.35	341	589	337	275	47.0	46.9	4.2

Data from the S1 ice samples of the present test series give an average flexural and elastic modulus of 4.00 ± 1.01 MPa and 6.02 ± 0.64 GPa at -5oC. Data at a nominal temperature of -0.2°C give an average flexural and elastic modulus of 2.28 ± 0.61 MPa and 4.16 ± 1.27 GPa.

Gow and Ueda (1989) presented results of 730 small-beam tests with laboratory grown S1 and S2 ice in temperatures ranging from -1°C to -19°C. Their data show that macrocrystalline (Sl) and columnar (S2) ice differs appreciably in their flexural characteristics and that these differences are attributable to variations in the size and orientation of the crystals in the ice and the thermal condition of the beams.

Han et al. (2016) examined the flexural strength and effective modulus of large columnar-grained freshwater ice in a small lake in Harbin, northern China, in the temperature range of −0.5°C to −10.0°C and strain rates of $4.6 \times 10^{-7}\ s^{-1}$ to $1.7 \times 10^{-3}\ s^{-1}$ under the same set-up (i.e., 3-point loading simple beams). The reported 830mm grain size at 5mm depth was comparable to the USCG samples. A re-analysis of their data using data in the brittle-ductile-transient range gives an average flexural strength and effective modulus of large columnar-grained freshwater ice at −5°C of 2.9 ± 0.3 MPa and 5.1 ± 0.8 GPa, respectively. (See Figure 6 of the cited reference.)

Dempsey et al. (1999) examined scale effects on the in-situ tensile strength and fracture of large grained S1 freshwater ice at Spray Lakes Reservoir, Alberta. The authors observed that laboratory-scale S1 data are extremely sensitive to specimen size after examining the existing apparent fracture toughness of S1 ice at laboratory-scale. Laboratory-scale uniaxial testing of S1 macrocrystalline ice was not feasible based solely on the diameter of approximately fifteen times the average grain size recommended for the tension-compression testing of cylinders of ice based on experimental evidence (Jones and Chew, 1981; Earle et al., 1984). Hence, the results were subjective to large size effect.

Data from the S1 ice samples of this series with simple beams tested at -5ºC give an average flexural strength and elastic modulus of 1.34 ± 0.04 MPa and 4.10 ± 1.53 GPa, respectively. Data at a nominal temperature of -0.2 ºC give an average flexural strength and elastic modulus of 0.82 ± 0.08 MPa and 2.32 ± 0.65 GPa, respectively.

Barrette (2011) conducted a laboratory investigation on the flexural strength of S2 ice harvested from the Rideau Canal, Canada. The data used for comparison are an average strength value of eight clear ice samples (see Table 1 of the cited publication).

Timco and O'Brien (1994) reviewed 2495 experimentally measured flexural strength data from 19 investigators. They reported no indication of a strong temperature influence on the strength of the freshwater ice at temperatures less than -4.5°C. All simple beam data for temperatures below -4.5°C were averaged to give a value of 1.73 ± 0.25 MPa. The data points corresponding to -1ºC and -0.2ºC are estimated from Figure 1 of the cited reference.

Compression Tests

Compression tests were conducted with loading both in horizontal (loading perpendicular to columnar grains) and vertical (loading parallel to grains) directions with specimens made from the four ice sample blocks. The structures of S1 and S2 ice are drastically different, resulting in a strength difference similar to that observed with the flexural strength as shown in Figure 7.

Table 3 summarizes the uniaxial compressive strength test results. Figure 7 shows a comparison between the present test series and Kirby (2007) compressive strength data. Figure 8 shows the uniaxial compressive strength of horizontally loaded S2 samples in comparison with data reported by Kirby (2007), Cole (1987), El-Tahan et al. (1984 and 1988), Gagnon and Gammon (1995), Meng and Guo (2015), Sinha and Frederking (1987), Qi et al. (2017), Lian et al. (2017), Jones (1982), Sinha (1982), Ramseier (1975), Dutta et al. (2004) and Kim and Keune (2007) with similar ice and loading conditions.

The compressive strength of ice in a horizontal loading direction is important, as when ice impacts rigid vertical structures it may fail in compression. The uniaxial compressive strength of all S2 ice reported in the datasets used for comparison are obtained in the horizontal loading direction, i.e. Qi et al (2017), Sinha (1982) and Dutta et al. (2004). The other datasets are granular ice, where the effect of loading direction is negligible, e.g., Cole (1987), El-Tahan et al. (1984, 1988), Gagnon and Gammon (1995), Sinha and Frederking (1987), Jones (1982), Ramseier (1975), and Kim and Keune (2007).

With the exception of Cole (1987), El-Tahan et al. (1984, 1988), Lian et al. (2017), Meng and Guo (2015), Kirby (2007) and the present test series, all previous tests were conducted with ice temperatures other than -5ºC. The data were normalized to -5ºC using Equation 2 prior to comparison. Equation 2 is based on the following equation based on Glen's law with an Arrhenius relationship (Barrette and Jordaan, 2003):

$$\dot{\varepsilon} = A(\sigma)^n exp\left(-\frac{Q}{RT}\right) \tag{1}$$

where $\dot{\varepsilon}$ is strain rate, σ is stress, A is a constant, n is the exponent of the power–law relationship taken as 4.63, the value for freshwater ice given in Figure 6 of Jones (2007), Q = 80 kJ/mol is the activation energy at the low confining pressures applicable to uniaxial test condition (Barrette and Jordaan, 2003), R = 8.31 J · mol^{-1} · K^{-1} is the universal gas constant and T is the absolute temperature.

Equation (1) can be re-written as:

$$\frac{\sigma_1}{\sigma_2} = exp\left[\frac{Q}{nR}\left(\frac{1}{T_1} - \frac{1}{T_2}\right)\right] \tag{2}$$

where the subscripts 1 and 2 refer to the strengths corresponding to two different temperatures.

Figure 8 shows the good correlation of the test results with Kirby's 2007 results, and the general trend exhibited with the other test data. It gives confidence of using data from general sources when data for a specific ice condition are not available as long as the ice parameters are within the specific range of test conditions.

The compressive strength of the S2 ice samples at -5ºC (e.g., 2.02 MPa) is 11% lower than those obtained in 2007 for the same ice (e.g., 2.265 MPa) loaded in the same direction by Kirby (2007). Please note that the Kirby (2007) tests were conducted with cylindrical samples, whereas we used square columns with comparable strain rates. Because the amount of strain to achieve compressive failure is very small (typically around 1%), that difference in configuration is not expected to have a significant influence on the test results. However, the slightly lower strain rate used in 2007 could explain the difference. Furthermore, the Kirby (2007) data show the compressive strength was 68% higher if loaded in the vertical direction rather than in the horizontal direction, whereas, the data in the present series are only 5% higher. The reason for the difference is not clear.

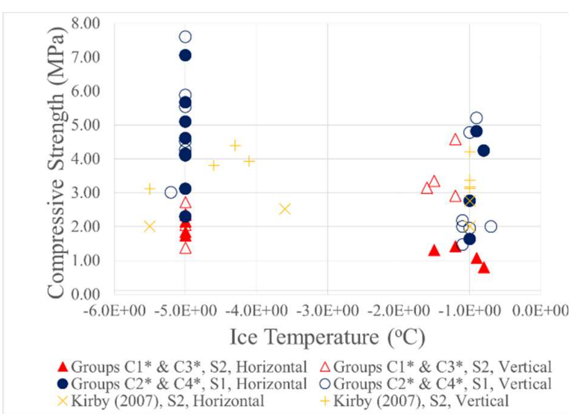

Figure 7 Summary of compressive strength in comparison with data reported by Kirby (2007).

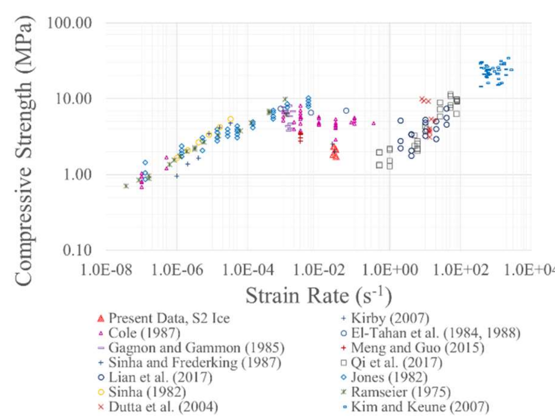

Figure 8 Uniaxial compressive strength of horizontally loaded S2 samples in comparison with data reported elsewhere on S2 freshwater ice

Table 3 Summary of compressive strength analysis on USCG Mackinaw ice samples: Loading speed = 4 mm/s, 1st C# – Cooler#, H# – Horizontal column #, 2nd C# – Vertical column #, * - 2 layers structure (to be continued in next page).

Column Sample	*Test Temp*	*Strain Rate*	*Peak Comp Strength*		*Max Load*	*Sample Length*	*Thick*	*Width*	*Density*
I.D.	(ºC)	(s^{-1})	(MPa)	(psi)	(kN)	(mm)	(mm)	(mm)	(kg/m^3)
C1H1	-5.0	3.0E-02	2.15	312	8.8	134.9	64.0	63.9	911.8
C1H2	-5.0	2.6E-02	2.35	340	12.7	152.8	73.4	74.0	904.4
C1H4	-5.0	2.6E-02	1.84	267	11.1	155.8	77.7	77.5	916.3
C3H2	-5.0	3.0E-02	1.74	252	7.9	132.4	67.6	66.9	913.4
C2H1*	-5.0	4.3E-02	3.12	452	5.5	93.6	42.1	41.9	916.8
C2H3*	-5.0	4.2E-02	5.66	821	11.8	94.2	45.4	45.8	919.3
C2H5	-5.0	4.3E-02	5.10	739	11.8	93.8	52.6	44.2	919.5
C2H7	-5.0	4.0E-02	2.29	332	4.6	99.4	44.4	45.2	913.7
C4H1*	-5.0	4.4E-02	4.14	601	8.4	91.9	45.1	45.1	913.2
C4H3*	-5.0	4.3E-02	4.10	594	7.2	92.3	42.0	42.1	914.6
C4H5	-5.0	4.6E-02	4.61	668	9.7	86.1	45.9	45.7	918.8
C4H7	-5.0	4.3E-02	7.06	1024	11.5	92.0	40.4	40.3	922.4
C1C1	-5.0	2.8E-02	2.37	344	13.4	141.1	75.1	75.1	917.4
C1C2	-5.0	3.1E-02	2.72	395	11.1	130.2	63.8	63.8	915.8
C3C1	-5.0	2.7E-02	1.38	200	7.7	149.6	74.7	74.6	917.4
C3C2	-5.0	2.8E-02	2.04	296	10.6	145.1	72.1	72.1	917.5
C2C1	-5.0	4.7E-02	4.51	654	8.0	85.0	42.2	42.2	918.2
C2C2	-5.0	4.5E-02	5.54	803	11.0	89.5	44.7	44.6	921.5
C2C7*	-5.2	4.5E-02	3.00	435	5.7	88.8	43.5	43.5	153.3
C2C8*	-5.0	4.0E-02	4.27	619	10.8	100.7	50.3	50.3	232.5
C4C2	-5.0	4.7E-02	7.60	1102	12.6	85.0	40.6	40.7	916.0
C4C3	-5.0	4.8E-02	5.88	852	9.9	83.1	40.9	41.2	913.6
C1H3	-0.8	3.0E-02	0.80	116	3.4	135.2	64.7	65.4	515.3
C1H6	-0.9	3.1E-02	1.07	156	4.5	130.1	64.9	64.7	501.6
C3H1	-1.2	2.7E-02	1.41	205	7.7	145.6	73.7	74.3	725.5
C3H3	-1.5	3.1E-02	1.31	189	5.3	127.5	64.5	63.5	475.8
C2H2	-1.0	5.0E-02	1.63	237	2.6	79.5	39.9	40.6	115.5
C2H6	-0.9	4.3E-02	4.81	697	8.4	92.4	41.8	41.9	146.4
C4H6	-0.8	4.1E-02	4.25	616	8.9	96.5	45.8	45.8	184.5
C4H7	-1.0	4.3E-02	2.75	399	6.7	93.6	49.4	48.9	206.5
C1C4	-1.2	3.0E-02	2.91	422	12.6	131.5	65.8	65.8	521.8
C1C5	-1.2	2.9E-02	4.58	665	24.1	138.3	72.5	72.5	668.5
C3C3	-1.6	2.6E-02	3.15	457	19.9	156.4	79.5	79.5	908.9
C3C4	-1.5	2.5E-02	3.35	486	18.5	161.1	74.4	74.3	815.5
C2C5	-1.1	4.4E-02	1.46	212	3.4	89.9	48.2	48.1	190.9
C2C6	-1.0	4.2E-02	1.95	283	4.2	96.0	46.2	46.0	186.5
C2C3*	-1.1	4.2E-02	2.17	315	3.9	94.4	42.4	42.2	154.3
C2C4*	-1.1	4.3E-02	1.99	289	4.6	93.6	47.9	47.8	195.9
C4C5	-0.7	4.9E-02	2.00	290	6.1	82.0	55.3	55.1	227.6
C4C6	-1.0	5.0E-02	4.77	692	12.1	79.2	50.4	50.5	185.4
C4C7	-0.9	4.3E-02	5.21	755	8.7	92.3	40.8	40.7	140.7

CONCLUSIONS

This paper documents the results of ice property analysis on the four ice samples harvested at three sites during the USCG's ice trials in March 2021 with its Great Lakes Icebreaker (GLIB) Mackinaw (WLBB-30). The trials were conducted on March 5th and 6th in the Green Bay area south of Chambers Island in Lake Michigan. The ice property analysis focuses on the flexural strength, compressive strength and crystal structure/size of the harvested samples.

Twenty-six flexural strength tests and 41 compressive strength tests were performed at two targeted ice temperatures of -5 ºC and -0.2 ºC (nominal) with a total of 65 tests. Kirby (2007) measured ice flexural and compressive strength from the Great Lakes using the same test set-up with similar sample size and ice temperature that affords direct comparison. The data are also compared with results reported elsewhere for similar ice and test conditions.

Through thickness vertical thin sections show a typical S2 columnar ice structure for two of the samples, i.e., Cooler1 and Cooler3, and a less common T3/S1 superimposed ice with macrocrystalline structure for the other 2 samples, i.e., Cooler2 and Cooler4. The difference in crystalline structure results in drastically different values for strength and elastic modulus between the S1 and S2 ice samples. The S1 ice has higher strength and elastic modulus than those of S2 ice. For example, at T=-5ºC, the average flexural strength for the S1 and S2 ice samples are 4.00 ± 1.01 MPa and 1.34 ± 0.04 MPa, respectively. The S1 ice is 2.98 times stronger than the S2 ice at this temperature. At T=-0.2ºC, the average flexural strength for the S1 and S2 ice samples are 2.28 ± 0.61 MPa and 0.82 ± 0.08 MPa, respectively. The S1 ice is 2.80 times stronger than the S2 ice. Furthermore, the average ice flexural strength of 1.34 MPa obtained at -5ºC for the S2 ice specimens are comparable to Kirby's 2007 data of the same ice type, i.e., 1.21± 0.2 MPa, obtained at the same temperature.

The compressive strength of the S2 ice samples at -5ºC (e.g., 2.02 MPa) is 11% lower than those obtained in 2007 for the same ice (e.g., 2.265 MPa) loaded in the same direction (Kirby, 2007). However, the 2007 data show the compressive strength was 68% higher if loaded in the vertical direction rather than in the horizontal direction; whereas, the data in the present series show only 5% higher. The reason for the difference is not clear.

The compressive strength of the S1 ice samples is consistently higher than that of the S2 samples, but with a larger data scattering, e.g., ranging from 2.29 MPa to 7.06 MPa for Cooler2 and Cooler4, which were from the same site. Nevertheless, the data still show a strength 2.23 times greater than that of S2 samples tested under the same horizontal loading condition and temperature of -5ºC. With the aforementioned uncertainty demonstrated by data scattering, the data still compare well with datasets from Han et al. (2016), Gow and Ueda (1989) and Dempsey et al. (1988) for S1 ice.

These data were also compared and found to be generally consistent with data from elsewhere, including the previous test programme (Kirby, 2007).

ACKNOWLEDGEMENTS

The author acknowledges the generous support of USCG for the collection of ice samples during its Great Lake ice trial, and their financial support of the laboratory analysis. The author also acknowledges Mr. Austin Bugden of NRC for his assistance in performance the ice property measurements.

REFERENCES

Barrette, P.D., and Jordaan, I.J., 2003. Pressure–temperature effects on the compressive behaviour of laboratory-grown and iceberg ice. Cold Regions Science and Technology, 36(1-3): 25–36.

Barrette, P.D., 2011. A laboratory study on the flexural strength of white ice and clear ice from the Rideau Canal Skateway. *Canadian Journal of Civil Engineering, 38*(12): 1435-1439.

Cole, D.M., 1987. Strain rate and grain-size effects in ice. Journal of Glaciology, Vol. 33, No. 115.

Dempsey, J.P., Nigam, D., .and Cole, D.M., 1988. The flexure and fracture of macrocrystalline S1 type freshwater ice. Proc. 7th International Conference on Offshore Mechanics and Arctic Engineering (OMAE), Houston, USA, pp. 39-46.

Dempsey, J.P., Defranco, S.J., Adamson, R.M., and Mulmule, S.V., 1999. Scale effects on the in-situ tensile strength and fracture of ice Part I: Large grained freshwater ice at Spray Lakes Reservoir, Alberta. International Journal of Fracture, 95(1): 325-345.

Dutta, P.K., Cole, D.M., Schulson, E.M., and Sodhi, D.S., 2004. A fracture study of ice under high strain rate loading. International Journal of Offshore and Polar Engineering, 14 (3): 182–188.

Earle, E.N., Frederking, R.M.W., Gavilo, V.P., Goodman, D.J., Hausler, F.U., Mellor, M., Petrov, I.G. and Vaudrey, K., 1984. IAHR-Recommendations on testing methods of ice. 4th report of working group on testing methods in ice. Proceedings of the 7th IAHR Symposium on Ice, Hamburg, Germany, Vol. IV, pp. 1–41.

El-Tahan, H., Swamidas, A.S.J., Arockiasamy, M., and Reddy, D.V., 1984. Strength of iceberg and artificial snow ice under high strain-rates and impact loads. Proc. 3rd OMAE, Vol. 3, ASME, New York, pp. 158–165.

El-Tahan, H., Swamidas, A.S.J., and Arockiasamy, M., 1988. Impact/indentation strength of iceberg and artificial snow ice. Offshore Mechanics and Arctic Engineering, 110: 87–93.

Gagnon, R.E., and Gammon, P.H., 1995. Triaxial experiments on iceberg and glacier ice. Journal of Glaciology. 41(139): 528–540.

Gow, A.J., and Ueda, H.T., 1989. Structure and temperature dependence of the flexural properties of laboratory freshwater ice sheets. Cold Reg. Sci. Technol., 16(3): 249–269.

Han, H.W, Jia, Q., Huang, W.F., and Li, Z.J., 2016. Flexural strength and effective modulus of large columnar-grained freshwater ice. Journal of Cold Regions Engineering, 30(2), 04015005.

Hitch, R.D., 1959. Flexural Strength of Clear Lake Ice. Technical Report 65, U.S. Snow, Ice and Permafrost Research Establishment, Corps of Engineer, Wilmette, Illinois.

Jones, S.J. and Chew, H.A.M., 1981. On the grain-size dependence of secondary creep. Journal of Glaciology, 27(97): 517–518.

Jones, S.J., 1982. The confined compressive strength of polycrystalline ice. Journal of Glaciology, 28(98):171–177.

Jones, S.J. and Chew, H.A.M., 1983. Effect of sample and grain size on the compressive strength of ice. Annals of Glaciology, 4: 129-132.

Jones, S.J., 2007. A review of the strength of iceberg and other freshwater ice and the effect of temperature. Cold Regions Science and Technology, 47: 256–262.

Kim, H., and Keune, J.N., 2007. Compressive strength of ice at impact strain rates. Journal of Materials Science, 42: 2802-2806.

Kirby, C., 2007. USCGC MACKINAW (WLBB-30) Ice Trials 07: Ice Properties Measurement Program. NRC Report Number TR-2007-28. Protected document, Limited Distribution. NRC-OCRE, St. John's, Canada.

Kirby, C., Barker, A., Barrette, P. and Frederking, R., 2021, USCG Mackinaw - 2021 Ice Strength Testing. National Research Council. Ottawa, 10 pp.

Lavrov, V.V., 1971. Deformation and Strength of Ice. Translated from Russian for the National Science Foundation by the Israel Program for Scientific Translations, 164p.

Lian, J., Ouyang, Q., Zhao, X., Liu, F., and Qi, C., 2017. Uniaxial compressive strength and fracture mode of lake ice at moderate strain rates based on a digital speckle correlation method for deformation measurement. Applied Sciences, 7 (5): 495.

Masterson, M., Graham, W.P., Jones, S.J., and Childs, G.R., 1997. A comparison of uniaxial and borehole jack test at Fort Providence Ice Crossing, 1995. Canadian Geotechnical Journal, 34 (3): 471 – 475

Meng, W. and Guo, Y., 2015. Experimental study on mechanical properties of ice. Proceedings of the AASRI International Conference on Industrial Electronics and Applications (IEA2015), London, UK, pp. 192-196.

Michel, B. and Ramseier, R., 1971, Classification of river and lake ice. Canadian Geotechnical Journal, 8(1), p. 38-45.

Murdza, A., Schulson, E., and Renshaw, C., 2020. Strengthening of columnar-grained freshwater ice through cyclic flexural loading. Journal of Glaciology, 66(258): 556-566.

Qi, C.F., Lian, J.J., Ouyang, Q.N., and Zhao, X., 2017. Dynamic compressive strength and failure of natural lake ice under moderate strain rates at near melting point temperature. Latin American Journal of Solids and Structures, 14(9): 1669-1694.

Ramseier, R.O., 1975. Growth and Mechanical Properties of River and Lake Ice. Thèse, Génie civil, Université Laval, Québec, 243 pp. Also Manuscript Report Series, No. 40, 1976, Department of the Environment, Ottawa, Canada.

Schwarz, J., Frederking, R., Gavrillo, V., Petrov, I.G., Hirayama, K.I., Mellor, M., Tryde, P., and Vaudrey, K.D., 1981. Standardized testing methods for measuring mechanical properties of ice. Cold Regions Science and Technology, 4: 245–253.

Sinha, N.K., 1982. Constant strain- and stress-rate compressive strength of columnar-grained ice. Journal of Materials Science, 17(3): 785-802.

Sinha, N.K., and Frederking, R., 1987. Preliminary observations on compressive strength, deformation and Poisson's ratio of iceberg ice. Workshop on Extreme Ice Features, Banff, NRC Technical Memorandum 141, NRCC 28003, pp. 413–426.

Timco, G.W., and Frederking, R., 1982. Comparative strengths of fresh water ice. Cold Regions Science and Technology, 6(1): 21-27.

Timco, G.W., and O'Brien, S., 1994. Flexural strength equation for sea ice. Cold Regions Science and Technology, 22(3): 285–298.

Wilson, J.T., Zumberge, J.H., and Marshall, E.W., 1954. A Study of Ice on an Inland Lake. Department of Defense, U.S. Army Corps of Engineers, Snow Ice and Permafrost Establishment, Report No. 5, 78 p.